Potential-field signatures of buried Precambrian basement in the Western Canada Sedimentary Basin

Article in Canadian Journal of Earth Sciences · October 2000

DOI: 10.1139/cjes-37-11-1453

Mark Pilkington
Natural Resources Canada

Potential-field signatures of buried Precambrian basement in the Western Canada Sedimentary Basin[1]

M. Pilkington, W.F. Miles, G.M. Ross, and W.R. Roest

Abstract: An internally consistent, levelled compilation of magnetic data is derived for Alberta and northeastern British Columbia. With Bouguer gravity data, this compilation is used to refine the definition of Precambrian basement domains within the Western Canada Sedimentary Basin. Magnetic data are draped at a constant distance above the mapped basement surface to reduce the effects of varying magnetic source depths. Automated interpretation methods that effectively map outlines of magnetic sources are used to characterize the internal structure of the domains and to aid in their delineation. The basement domain map thus derived differs from previous interpretations in the extension of domains further to the southwest, due mainly to the availability of new public-domain magnetic data and the more precise definition of domain boundaries, based on the magnetic source location maps. The Nahanni, Hottah, Chinchaga, Thorsby, Vulcan, and Kiskatinaw domains are weakly magnetic and characterized by magnetic sources that are paramagnetic, comprising low-susceptibility silicate minerals. All other domains are characterized by the presence of ferrimagnetic material, most likely magnetite, which has a sufficiently high susceptibility to produce measurable anomalies. The largest anomalies and magnetizations are found in the Fort Nelson, Fort Simpson, Buffalo Head, Talston, Ksituan, and Matzhiwin domains. Such large magnetizations are usually indicative of intermediate igneous rocks associated with magmatic arc environments. Moderate-amplitude anomalies and (or) magnetizations are characteristic of the Nova, Wabamun, Lacombe, Rimbey, Loverna, and Medicine Hat domains, suggesting the presence of ferrimagnetic basic and granitoid rocks. Within some of the moderately magnetic domains are areas of paramagnetic lithologies that produce no magnetic anomalies. The narrower regions of magnetic lows, such as the Thorsby, Kiskatinaw, and Vulcan domains, are interpreted as resulting from demagnetization effects accompanying collision. Since demagnetization zones are limited in areal extent, the wider, more extensive magnetic lows of the Chinchaga and Hottah domains likely result from a combination of boundary demagnetization and a lower bulk magnetization level of crustal lithologies present.

Résumé : Des données magnétiques lissées et concordantes ont été compilées pour l'Alberta et le nord-est de la Colombie-Britannique. Avec les données de gravité Bouguer, cette compilation est utilisée pour préciser la définition des domaines du socle Précambrien dans le bassin sédimentaire de l'Ouest canadien. Les données magnétiques sont ramenées à une distance constante au-dessus de la surface cartographiée du socle afin de réduire les effets de sources magnétiques à des profondeurs variables. Des méthodes d'interprétation automatisées qui cartographient de façon efficace les contours de sources magnétiques sont utilisées pour caractériser la structure interne des domaines et pour aider à les délimiter. La carte du domaine du socle ainsi définie diffère des interprétations antérieures par l'extension des domaines plus loin vers le sud-ouest, surtout en raison de la disponibilité de nouvelles données magnétiques maintenant publiques et de la définition plus précise des limites des domaines basées sur les cartes de localisation des sources magnétiques. Les domaines de Nahanni, Hottah, Chinchaga, Thorsby, Vulcan et de Kiskatinaw sont faiblement magnétiques et ils sont caractérisés par des sources magnétiques qui sont paramagnétiques et qui comprennent des minéraux silicatés de faible susceptibilité. Tous les autres domaines sont caractérisés par la présence d'un matériau ferrimagnétique, fort probablement de la magnétite, qui a une susceptibilité suffisamment élevée pour produire des anomalies mesurables. Les plus grandes anomalies et magnétisations se retrouvent dans les domaines de Fort Nelson, Fort Simpson, Buffalo Head, Talston, Ksituan et de Matzhiwin. De telles grandes magnétisations indiquent généralement des roches ignées intermédiaires associées à des environnements d'arcs magnétiques. Des anomalies et (ou) magnétisations d'amplitude modérée caractérisent les domaines de Nova, Wabamun, Lacombe, Rimbey, Loverna et de Medicine Hat et sont des indices favorables pouvant indiquer la présence de roches granitoïdes et ferrimagnétiques basiques. À l'intérieur de quelques domaines modérément magnétiques se retrouvent des régions de lithologies paramagnétiques qui ne produisent pas d'anomalie magnétique. Les régions plus étroites de creux magnétiques tels que les domaines de

Received August 30, 1999. Accepted February 8, 2000. Published on the NRC research press Web site on October 19, 2000.
Paper handled by Associate Editor L. Corriveau.

M. Pilkington[2], W.F. Miles, and W.R. Roest. Geological Survey of Canada, 615 Booth Street, Ottawa, ON K1A 0E9, Canada.
G.M. Ross. Geological Survey of Canada, 3303–33rd St. NW, Calgary, AB T2L 2A7, Canada.

[1]Geological Survey of Canada Contribution 1999106. Lithoprobe Publication 1187.
[2]Corresponding author (e-mail: mpilking@nrcan.gc.ca).

Thorsby, de Kiskatinaw et de Vulcan sont interprétées comme étant le résultat d'effets de démagnétisation suivant une collision. Puisque les zones démagnétisées ont une étendue limitée, les creux magnétiques plus larges et plus extensifs des domaines de Chinchaga et de Hottah résultent probablement de la combinaison d'une démagnétisation aux limites et d'un niveau de magnétisation massique plus faible des lithologies crustales présentes.

[Traduit par Rédaction]

Introduction

As potential-field compilations extend to greater scales, they are used increasingly to tie existing isolated interpretations or maps together through continuous data coverage (e.g., Cady 1989; Percival et al. 1992), provide continent-scale (plate-tectonic) perspectives on geologic structure and evolution (Thomas et al. 1988; Hoffman 1989; Shaw et al. 1996), and extend geological mapping of exposed (particularly Precambrian basement) regions into sediment-covered areas (Coles et al. 1976; Ross et al. 1991; Johnson and Stewart 1995; Adams and Keller 1996; Leclair et al. 1997). A fundamental building block in these interpretations is the geophysical domain, distinguished on the basis of anomaly trend, texture, and amplitude. Where basement is exposed, these domains often coincide with lithotectonic domains, geologic provinces, or cratons, depending on the scale of investigation. Delineating areas of geophysical anomalies having similar characteristics is intended, therefore, to isolate areas of crust having similar lithological, metamorphic, and structural character, and possibly, history. Anomaly trends may indicate the type of deformation undergone; for example, sets of parallel, narrow curvilinear anomalies may attest to penetrative deformation, while broad ovoid anomalies might suggest relatively undeformed plutons. The average anomaly amplitude within a domain reflects its bulk physical properties. For example, calc-alkaline magmatic arcs generally are marked by belts of high-amplitude positive magnetic anomalies, while greenstone terranes are commonly associated with subdued magnetic fields. In particular, attention is focussed on those geophysical signatures that most closely reflect the tectonic and (or) structural character of the domain. Additionally, where anomaly trends show abrupt changes in direction at domain boundaries, the relative age of the adjacent domains may also be inferred (Thomas et al. 1988; Wellman 1998).

Gravity data have been used successfully to map domains on a continental scale (e.g., Wellman 1985; Thomas et al. 1988). Gravity anomalies reflect density variations, both vertically and horizontally, throughout and below the whole crustal section. Long-wavelength anomalies can be caused by deep-seated isostatic effects, while shorter wavelength features can result from density changes in sedimentary rocks overlying crystalline basement (Sprenke and Kanasewich 1982; Stephenson et al. 1989). Due to the more rapid fall-off rate of magnetic fields compared with gravity and because most unmetamorphosed sedimentary rocks can be considered magnetically transparent at regional scales, magnetic anomalies reflect more closely the nature of the basement in covered regions. Magnetic data provide, therefore, the primary tool used below in defining domains in the Alberta and British Columbia basement.

Ross et al. (1991) and Villeneuve et al. (1993) subdivided the Precambrian basement of the Western Canada Sedimentary Basin (WCSB) in Alberta and northeastern British Columbia into domains based on a combination of potential-field data and age determinations of drill cores from basement intersections. Corroboration of their interpretation was provided by analogy with geophysical signatures of exposed geologic subdivisions of the Canadian Shield and the earlier subdivisions of Hoffman (1989). Ross et al. (1991) used proprietary, unpublished aeromagnetic data for the southern half of Alberta and located domain boundaries qualitatively, using the zero contour of the residual magnetic field as a proxy for the magnetic source body edges combined with anomaly character. Here, we extend and refine the earlier basement subdivision based on the present availability of public-domain aeromagnetic data coverage over the WCSB. Besides standard qualitative enhancements of the data, such as derivatives and shaded relief maps, quantitative methods are used to emphasize the internal character of the domains and more accurately define their boundaries.

Magnetic data preparation

Aeromagnetic survey coverage of the WCSB varies widely in terms of data quality, line spacing, and flight height. Although magnetic data have been acquired over much of the area, particularly by the oil industry, public-domain data were limited to ~60% coverage until the advent of the Geological Survey of Canada – industry consortium that assembled in 1989 to fill most of the existing gaps. This program consisted of regional aeromagnetic surveys acquired over the period 1990–1992, with data publicly available by 1998. Figure 1 shows the distribution of data presently available over the WCSB and highlights the variety of survey types present. Flight-line spacing varies from 402 m to 6436 m, with most pre-1980 surveys having a 3.2–4.0 km interval and those post-1980 having a 1.6 km spacing. Data quality spans the spectrum from digitized hand-contoured, photographically located analogue data from the 1950s to recently acquired, digital, GPS-located, high-resolution survey data. The two survey modes used in the WCSB area (Fig. 1) are constant barometric altitude, where the aircraft flies at a constant altitude above mean sea level, and mean terrain clearance (or drape-flown), where surveys are flown at a constant height above the terrain.

The levelling of aeromagnetic surveys covering the WCSB to a common datum and to each other is required to account for secular variations in the geomagnetic field, arbitrary magnetometer base levels, variable flight-line spacing, and differences in flying height. This levelling has been achieved in several steps. Initially, residual magnetic field anomalies are calculated by subtracting the geomagnetic ref-

Fig. 1. Aeromagnetic survey distribution for Alberta and northeastern British Columbia. Note: 1 mile = 1609 m.

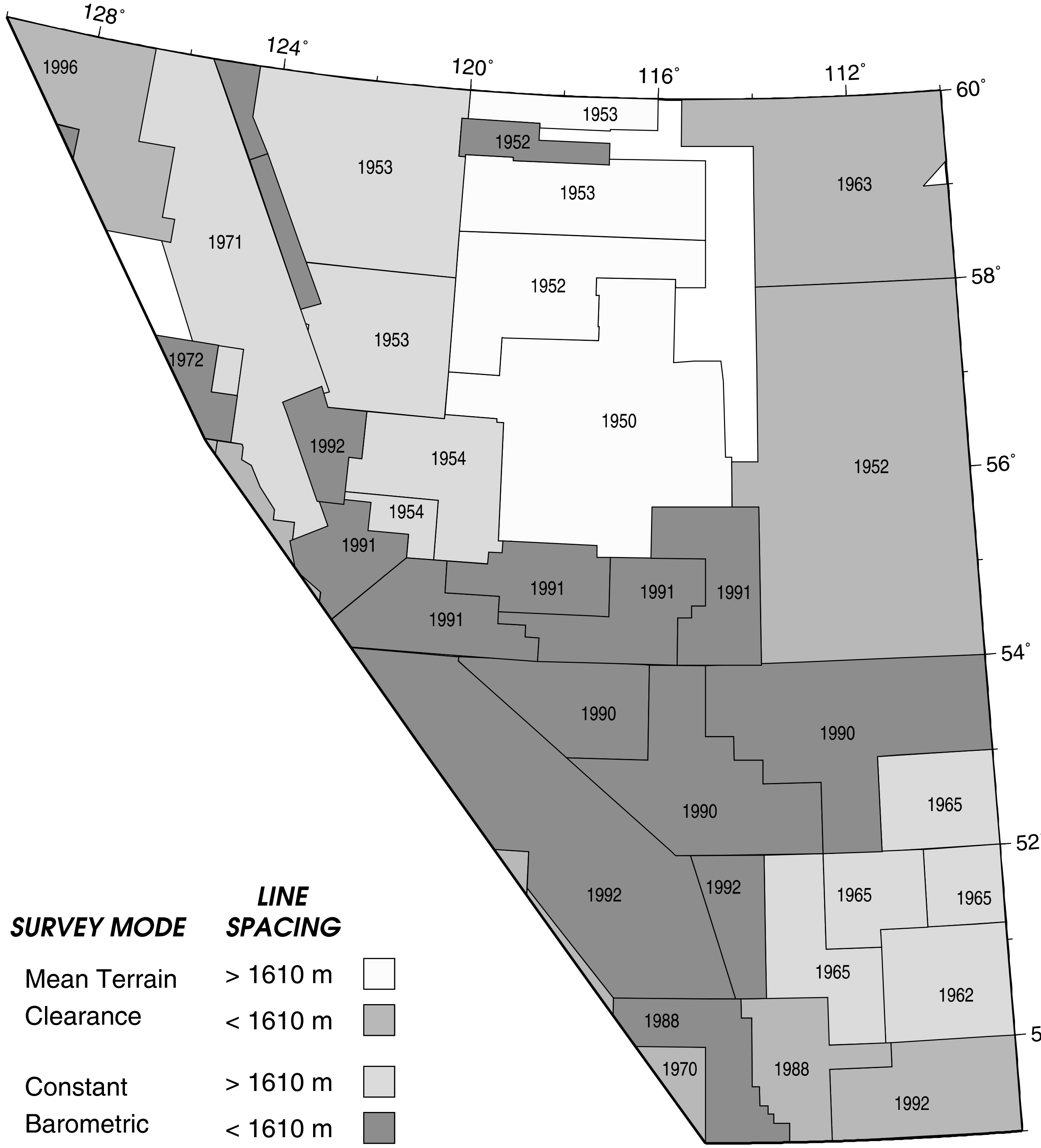

erence field appropriate to the survey epoch. Linking of the drape-flown aeromagnetic grids to the constant barometric altitude survey grids was then achieved by continuing or draping of the constant-altitude surveys onto a surface, 305 m (1000 ft) above the terrain, to remove the effects of variable flight height. Draping the data onto a surface of variable elevation rather than a constant-altitude (flat) surface is preferred, because it provides better resolution of anomalous features. A surface draped over the terrain will always be closer to the magnetic sources than a constant-altitude surface that is limited to being above the highest ground elevation in the survey area. At first, the draping was attempted by specifying a draping surface at a constant height above a digital terrain model. This method introduced noise into the resulting grids due to the presence of steep gradients in the surface topography and was deemed unsuccessful in merging of adjacent surveys. Later, a surface simulating an aircraft flying with a maximum 5% slope was

Fig. 2. Comparison of draping surfaces. Dashed line denotes a surface at a constant 305 m (1000 feet) above ground level. Solid line is the same surface restricted to a maximum 5% slope. The latter slope is, in places, much higher than the former due to the presence of higher topography perpendicular to the profile shown here.

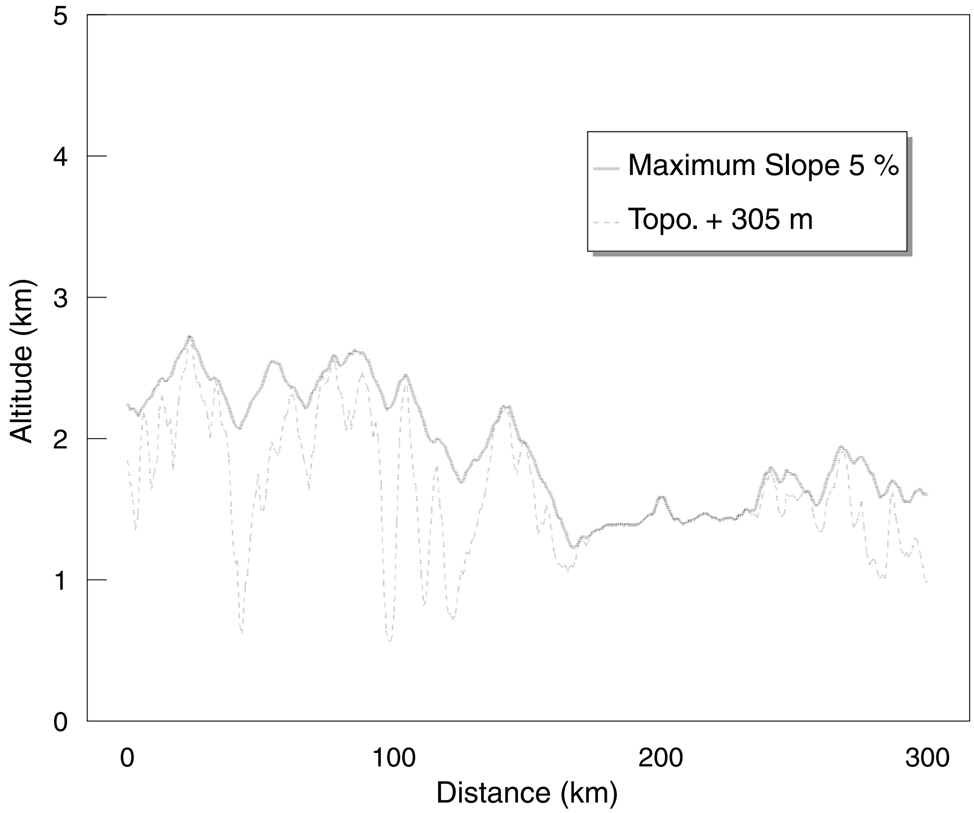

calculated (Fig. 2) and used as the draping surface, which greatly improved the quality of the merged surveys. The method used for draping of the constant-altitude surveys is based on a Taylor series expansion of the magnetic field on the measurement surface (Pilkington and Roest 1992). This approach was evaluated in areas where coincident drape-flown and constant-altitude survey data are available. The computational draping method compared well to the drape-flown data (Pilkington et al. 1995), validating its use in the levelling of the WCSB area.

Following the draping, digital surveys (post-1980) were levelled together by simply applying base-level shifts to the gridded data. Such shifts were usually <100 nT. Analogue surveys (pre-1980) required the removal of up to a third-order polynomial surface to match at survey boundaries. Having achieved an acceptable match of the long-wavelength anomaly components, the short wavelengths were matched at survey boundaries using a three-stage procedure. First, the difference between the target survey to be matched and the surrounding survey grids was found over their common overlap (usually <1 km). Second, the target survey perimeter was cut back a further 1–3 flight-line spacings and all grid values within this region set to zero. Third, the gap between the difference strip and the nulled grid was interpolated using minimum curvature to produce a smooth join between the two. These interpolated values then constituted the short-wavelength corrections added to the target grid. All grid corrections thus determined were then applied to the original profile data, which were subsequently gridded at a 400 m interval.

To remove the effects of the nonvertical geomagnetic field over the survey area, the data were reduced to the pole using values of 22°E and 76.5°N for the declination and inclination, respectively. Over the study area, the declination varies from 16° to 29°E and the inclination changes from 72.5° to 81.3°N. However, tests showed that using constant values over the whole area leads to a maximum of <1 km displacement in anomaly positions. For the reduction to the pole, we have implicitly assumed that any remanent magnetization present is small compared to the induced magnetization component or that it is aligned in the direction of the present-day geomagnetic field (Watkins 1961). The latter is the case for viscous remanent magnetization, which is usually acquired in or subparallel to the present field direction. The presence of viscous remanent magnetization becomes more important at greater depths and temperatures, and it could represent, on average, 20–25% of the total magnetization present (Shive 1989; Clark 1997). The predominance of induced magnetization effects produced by the present-day field is expected because it is unlikely that coherent thermal remanent magnetization directions would exist over distances comparable to the domain sizes (Arkani-Hamed and Celleti 1989). Formation and cooling of large, particularly plutonic, masses have likely taken place over time periods much larger than the average geomagnetic polarity interval (Schlinger 1985; Shive 1989). Hence, the cancelling effect of different thermal remanent magnetization directions leads to a diminished remanent contribution to the observed magnetic field. Thermal remanent magnetization effects, however, may be important at smaller length scales (e.g., Clark

Fig. 3. Magnetic data after reduction to the pole using a constant value for the geomagnetic field inclination of 76.5°N and 22°E for the declination.

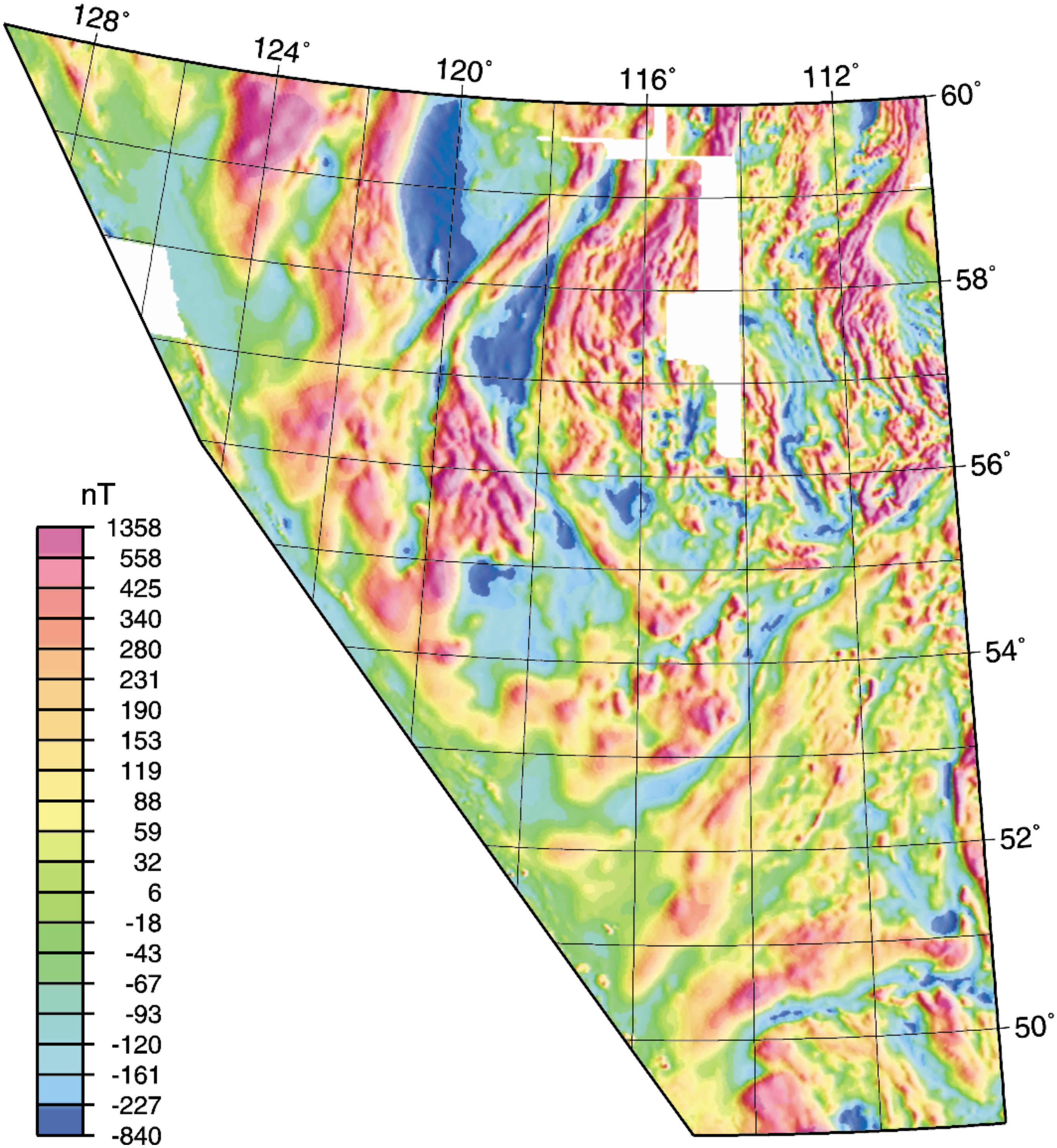

1997). Figure 3 shows the reduced-to-the-pole magnetic data that is the starting point for interpretation and further enhancement.

Gravity data

Figure 4 shows the Bouguer gravity data over the WCSB and Alberta, where the station spacing varies up to ~13 km. The gravity field is dominated by the long-wavelength anomaly low over the Cordillera caused by increased crustal thickness. This produces a gradual increase in gravity values toward the northeast that masks the more subtle anomalies present. Computing the horizontal gradient of the Bouguer gravity effectively suppresses the longer wavelength anomaly components and emphasizes the effects of density contrasts in the upper crust (Fig. 5).

Fig. 4. Bouguer gravity data for Alberta and northeastern British Columbia. Contour interval 5 mGal. Solid white lines denote interpreted domain boundaries.

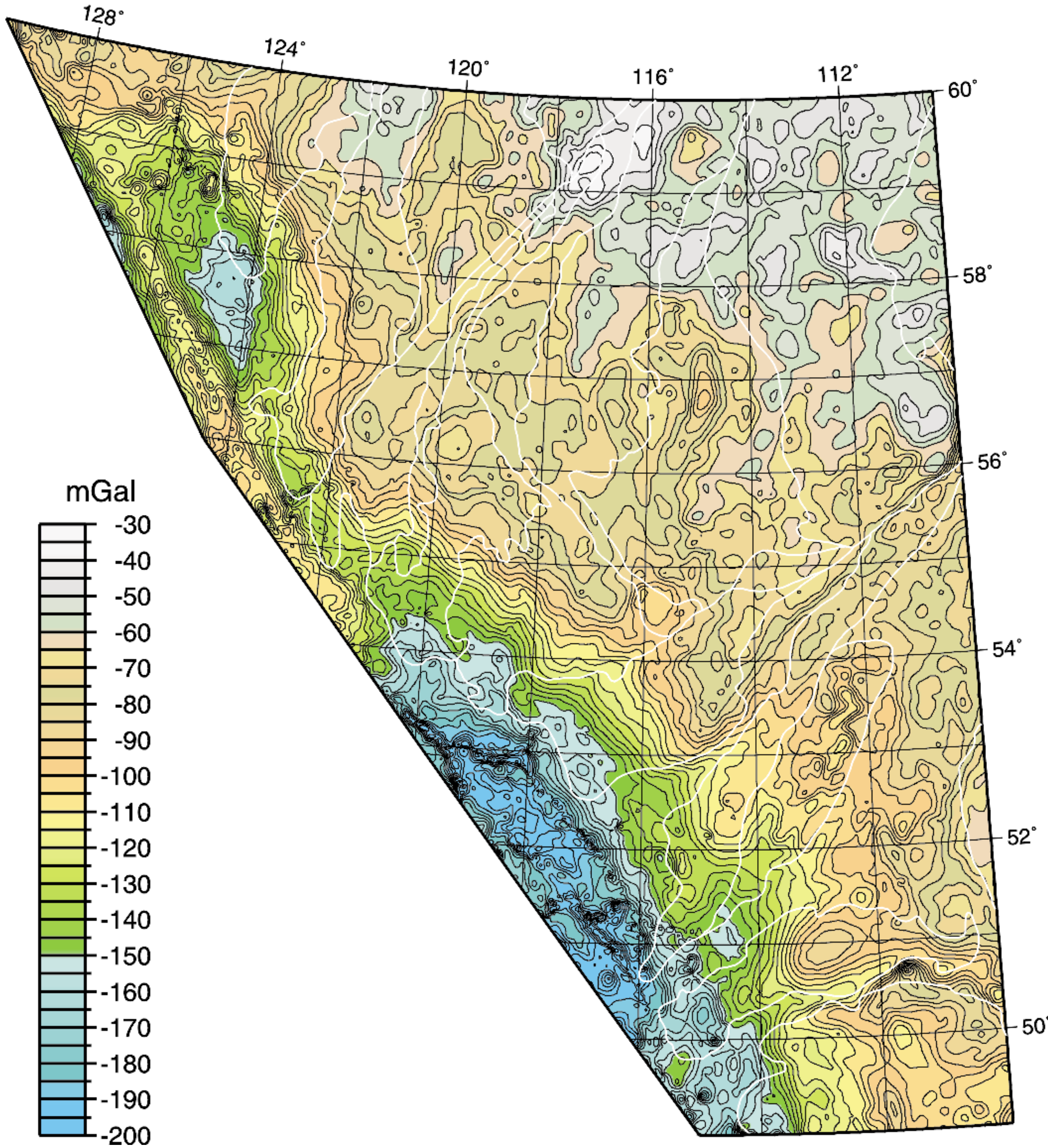

Magnetic data enhancement

The predominant effect of the increasing sediment thickness in the Western Canada Sedimentary Basin is to attenuate and broaden anomalies caused by magnetized sources in the basement. The general shape of the sedimentary cover in the WCSB approximates a westward-thickening wedge that increases in thickness from zero in northeast Alberta to more than 5 km in western Alberta. To reduce the effects of changes in the WCSB thickness on the different domain attributes, the observed magnetic field was draped onto a surface at a constant 1 km above the mapped Precambrian basement. In this way, the decrease in amplitude and increase in wavelength of anomalies caused by increasing

Fig. 5. Horizontal gradient of Bouguer gravity. Solid white lines denote interpreted domain boundaries.

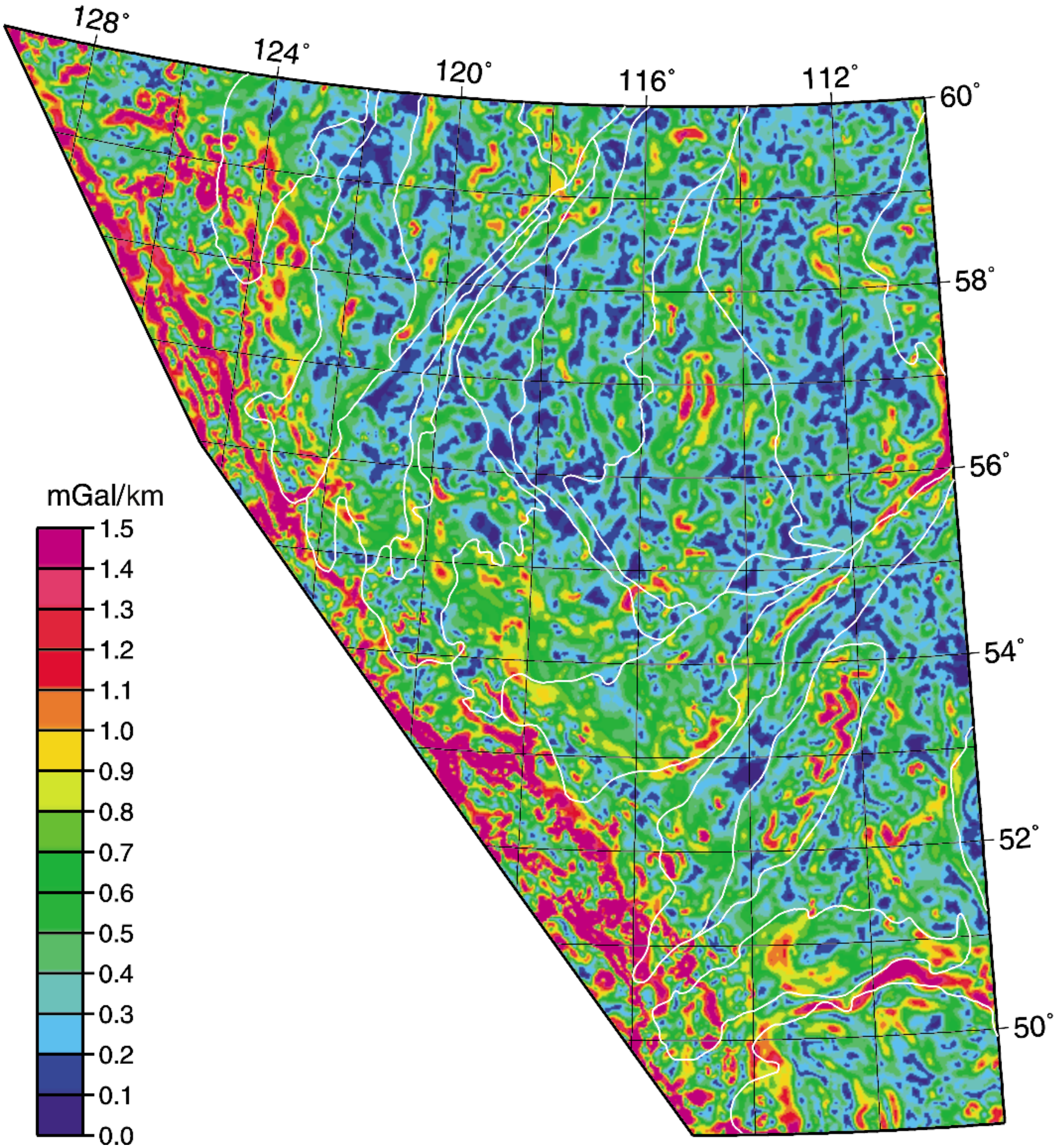

depth to sources over the WCSB is accounted for and the resulting anomalies are related entirely to source character within a particular domain and are not influenced by the thickness of the sedimentary cover. Again, the Taylor series method (Pilkington and Roest 1992) was used for the draping with basement depths (Fig. 6) based on gridding measured depths based on available drill hole basement intersections. Figure 7 shows the draped aeromagnetic data.

Draping results in improved resolution of anomalies in the deeper parts of the basin, where data are downward continued, and some smoothing (from upward continuation) in areas where the basin is <1 km thick. Note that, close to the western edge of the map area, high-amplitude anomalies caused by shallow Cordilleran plutonic and (or) volcanic rocks are caused by effectively continuing the field through the sources, leading to oscillations in the resulting field.

Fig. 6. Depth to Precambrian basement based on drill-hole data. Contour interval 200 m.

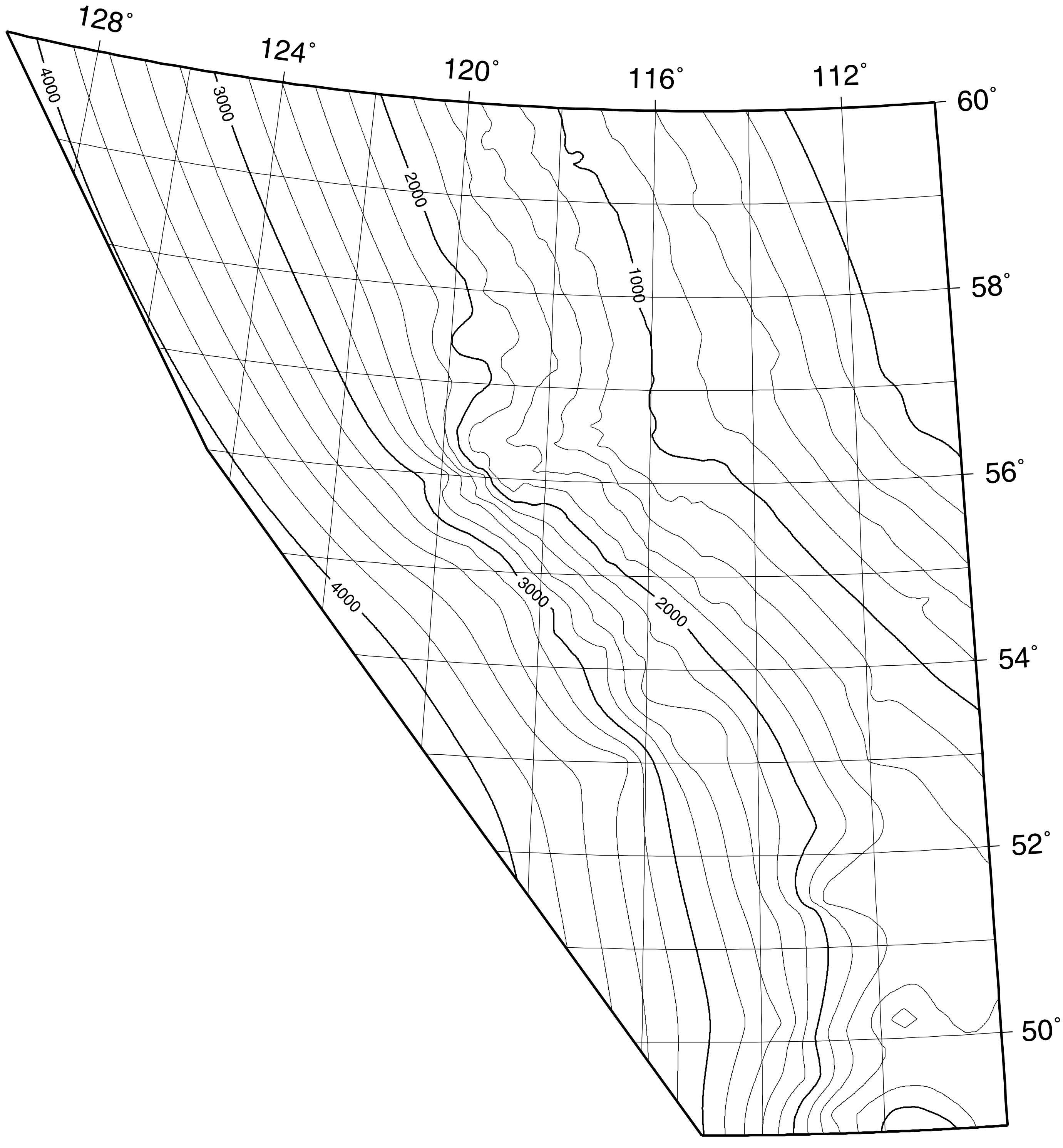

These processing artefacts have not been removed since our primary interest is in the field produced by the underlying basement. The draping also emphasizes some low-amplitude, short-wavelength anomalies (e.g., around 50.5°N, 115°W) that parallel the Cordilleran deformation front and are likely intrasedimentary in origin, occurring within the Cordilleran thrust belt. Longer wavelength trends associated with the deepening crystalline basement can be traced westward well over 100 km from the Cordilleran deformation front beneath the thrust sheets of the eastern Cordillera up to the Rocky Mountain Trench. Cook et al. (1995) even suggest that some east-trending features related to basement extend into the Omineca Belt west of the Rocky Mountain Trench. Wherever the western boundary of Canadian Shield

Fig. 7. Magnetic data of Fig. 3 after draping onto a surface 1 km above basement surface defined in Fig. 6. Solid white lines denote interpreted domain boundaries. Longer dashed line is the Cordilleran deformation front. Shorter dashed line is the edge of the Phanerozoic.

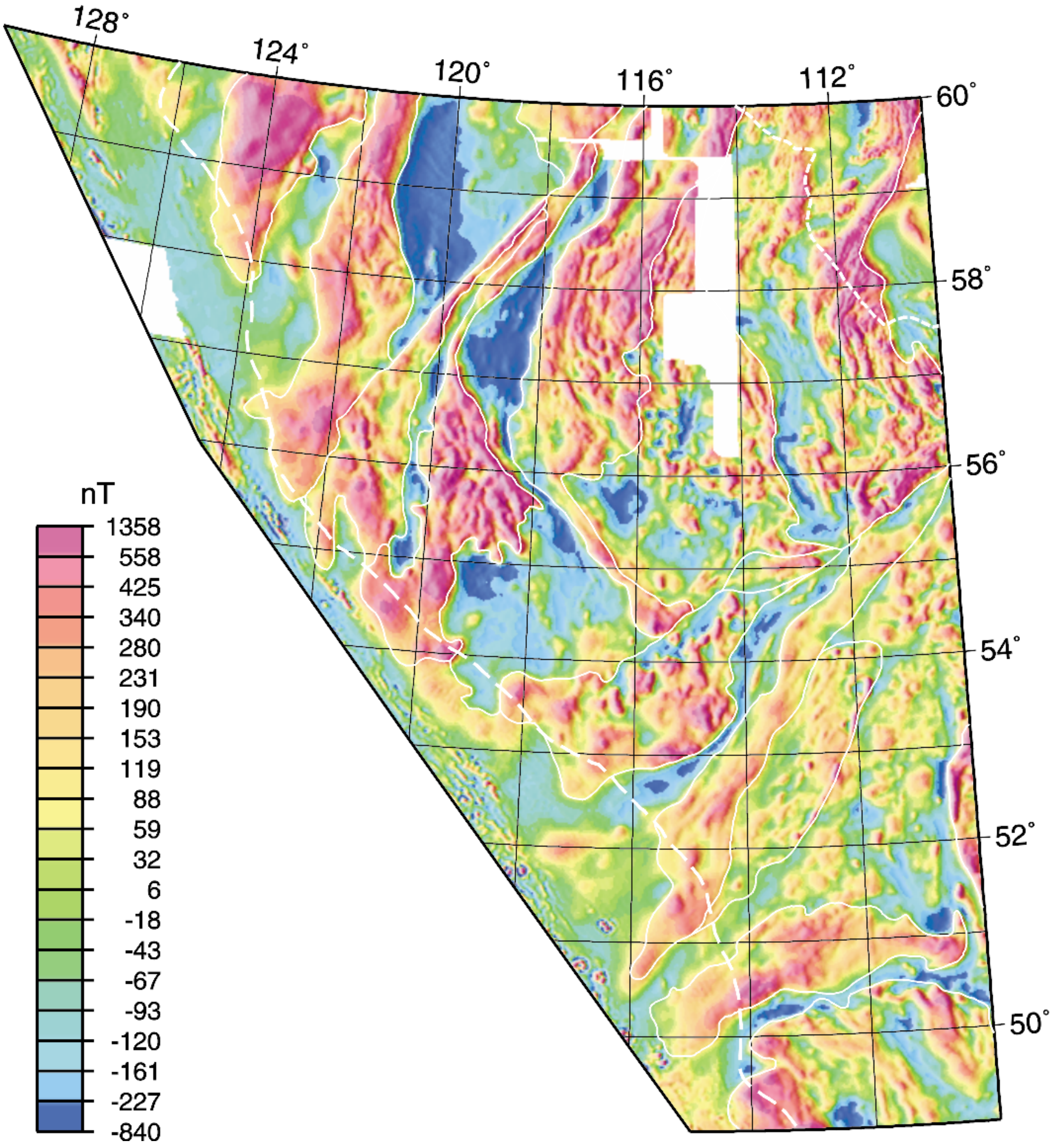

rocks is, their detection west of the Cordilleran deformation front is a strong affirmation of the thin-skinned nature of the thrust belt.

Domain definition

Characterizing geophysical domains relies heavily on anomaly attributes that are assumed to be indicative of the mode of formation, structure, and deformation history (Wellman 1985, 1998; Shaw et al. 1996). However, variable source depths within a domain may also contribute significantly to changes in anomaly shape and size. Draping over the basement does not take into account such variations. Therefore, to keep this effect to a minimum, we rely primarily on mapped source distributions within the basement rather than the mapped anomalies they produce (cf. Thomas et al. 1988) to characterize the different domains. Three techniques, Euler deconvolution, pseudo-gravity gradient, and analytic signal were applied to the gridded data to explore the source structure in the basement. Each method maps the edges of magnetized bodies or equivalently, lateral contrasts in magnetization, which are caused mainly by lithological and structural changes in the buried basement. Recognizing the limitations of the methods as discussed below, maps of the source edges are initially used to group trends that have similar orientation and spacing. Domain boundaries are then roughly delineated by areas of parallel or subparallel trends that have comparable anomaly amplitudes. The boundaries are then mapped more accurately using the source edge maps by placing margins at the positions of source edges coinciding with major amplitude changes. Figure 8 shows basement domains defined from potential-field data and their enhancement (Figs. 3–10), and the previous work of Ross et al. (1991). A detailed description of magnetic character, age, and type of domain is given in Villeneuve et al. (1993) and is summarized here in Table 1.

Euler deconvolution

Euler deconvolution is a semi-automatic technique that estimates magnetic source locations in three dimensions (Reid et al. 1990). The method involves the specification of two variables: window size and structural index. The window size used was 11.2 km, chosen to span the range of anomaly wavelengths and expected source depths. A structural index (SI) of zero was specified, which is appropriate for magnetic sources that can be described in terms of geologic contacts, that is, abrupt lateral changes in magnetization. As source depths increase, an SI of zero is not strictly applicable and higher values for SI should be used, which give deeper estimates. Furthermore, with more than one type of magnetic source body present, different values of SI may prove more appropriate in locating the various source bodies in a given area. However, to avoid the problems with specifying varying SI values over the study area, we used a constant value and note that the derived source depths generally represent a lower bound on the possible values. The Euler technique responds primarily to gradients in the data and in plan form effectively traces the (upper) edges of the source bodies. The horizontal coordinates of the source estimates are generally more reliable than the vertical, so they can be used alone for the delineation of structural and (or) lithological trends. For example, McDonald et al. (1992) interpreted major Euler solution trends from gravity and magnetic data in Wales as defining fault-bounded blocks within the Precambrian basement.

Figure 9 shows the magnetic source estimates for the WCSB based on the undraped data of Fig. 3. The general trend in source depths follows the increase in depth of the crystalline basement towards the Cordillera. The western boundary of the map indicates shallow sources occurring within the southern Cordillera. Exceptions to the westerly deepening source trend occur in the Rimbey domain, which shows deeper sources; the Lacombe domain (especially along its southern edge), which indicates shallower sources; and the Ksituan domain, which exhibits shallower sources in the region of the Peace River Arch. We also note deeper source depths occurring within the Athabasca basin.

Pseudo-gravity gradient

The pseudo-gravity gradient technique locates edges of magnetic source bodies after a transformation in the frequency domain that converts magnetic anomalies, reduced to the pole, into equivalent gravity anomalies (Cordell and Grauch 1985). After the transformation, steeper (horizontal) pseudo-gravity gradients tend to occur over the edges of causative bodies. If a body edge is vertical and sufficiently far from the effects of other interfering bodies, then the maximum gradient is located exactly above this edge. If the body edge dips, then the gradient maximum migrates in the downdip direction. Hence, computing the horizontal gradient of a pseudo-gravity map, followed by selection of the maxima, is an efficient way of "mapping" body edges (i.e., lateral pseudo-density contrasts correspond to lateral changes in magnetization). Wadge and Snoke (1991) used pseudo-gravity gradient maxima to revise and (or) confirm mapping of contacts and faults during geologic mapping. Cordell and Grauch (1985) and Hildenbrand (1985) used pseudo-gravity gradient maxima to help define the internal character and boundaries of basement geophysical terranes in sediment-covered regions. In some cases, the maxima location will migrate from the edges toward the centre of the body as the depth-to-source increases and the pseudo-gravity gradient (and the analytic signal discussed in the next section) does not resolve the individual edges of a deeply buried source body. As a rule of thumb, this effect occurs when the width of the body is less than its depth of burial. Figure 10*a* shows the mapped positions of pseudo-gravity gradient maxima derived from the draped magnetic data (Fig. 7). The pseudo-gravity transformation involves an integration of the magnetic field data, leading to some smoothing of the field and accompanying loss in resolution. In areas where source bodies are close to one another, the pseudo-gravity gradient does not resolve individual edges so we have calculated the horizontal gradient maxima for the magnetic field itself (Fig. 10*b*). Due to the profile shape of the magnetic field produced by a geologic contact, the horizontal gradient maxima will also occur at locations that parallel the source edge. Hence, not all trends in Fig. 10*b* coincide with source edges, however the higher resolution of the trend distribution is apparent.

Locations of gradient maxima for the gravity data of Fig. 5 are given in Fig. 10*c*. In an equivalent fashion to the magnetic data, these maxima define lateral density contrasts.

Analytic signal

The analytic signal of a magnetic anomaly is a combination of the vertical and horizontal magnetic gradients (Roest et al. 1992). It has the useful property of being independent of the magnetization direction of the causative body. As in the case of the pseudo-gravity gradient, the analytic signal exhibits a maximum at the edge of a magnetic source body. Theoretically, variation in dip along the edges has no effect on the location of the maximum. Hence, computing the analytic signal and locating its maxima is an efficient way of mapping the edges of magnetic bodies independent of magnetization orientations and dipping contacts. Figure 10*d*

Fig. 8. Precambrian basement domains of Alberta and northeastern British Columbia based on Ross et al. (1991), Villeneuve et al. (1993), and this work. Abbreviation: STZ, Snowbird tectonic zone.

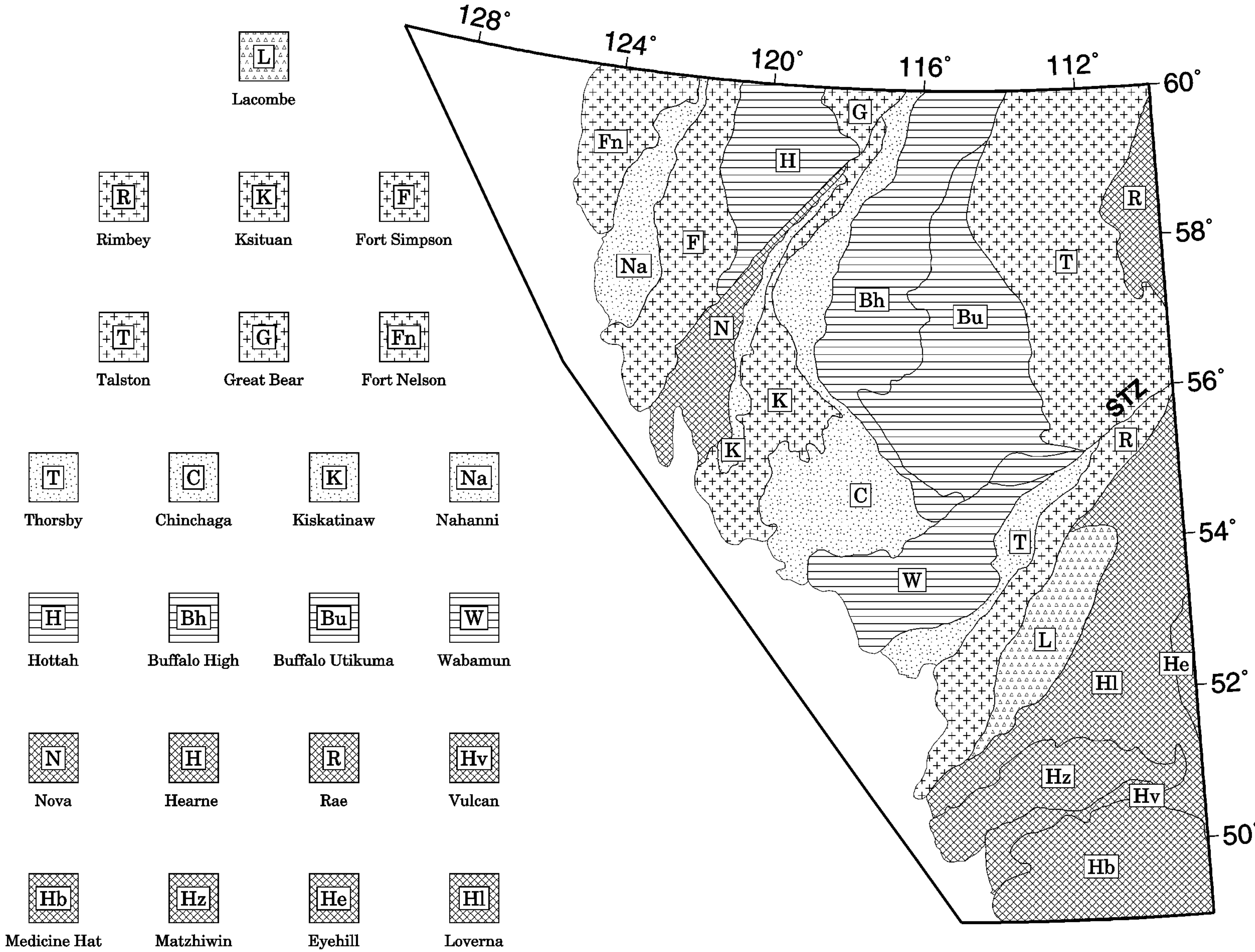

Fig. 9. Magnetic source locations estimated using Euler deconvolution. Solid lines denote interpreted domain boundaries. Inset shows histogram of computed depths.

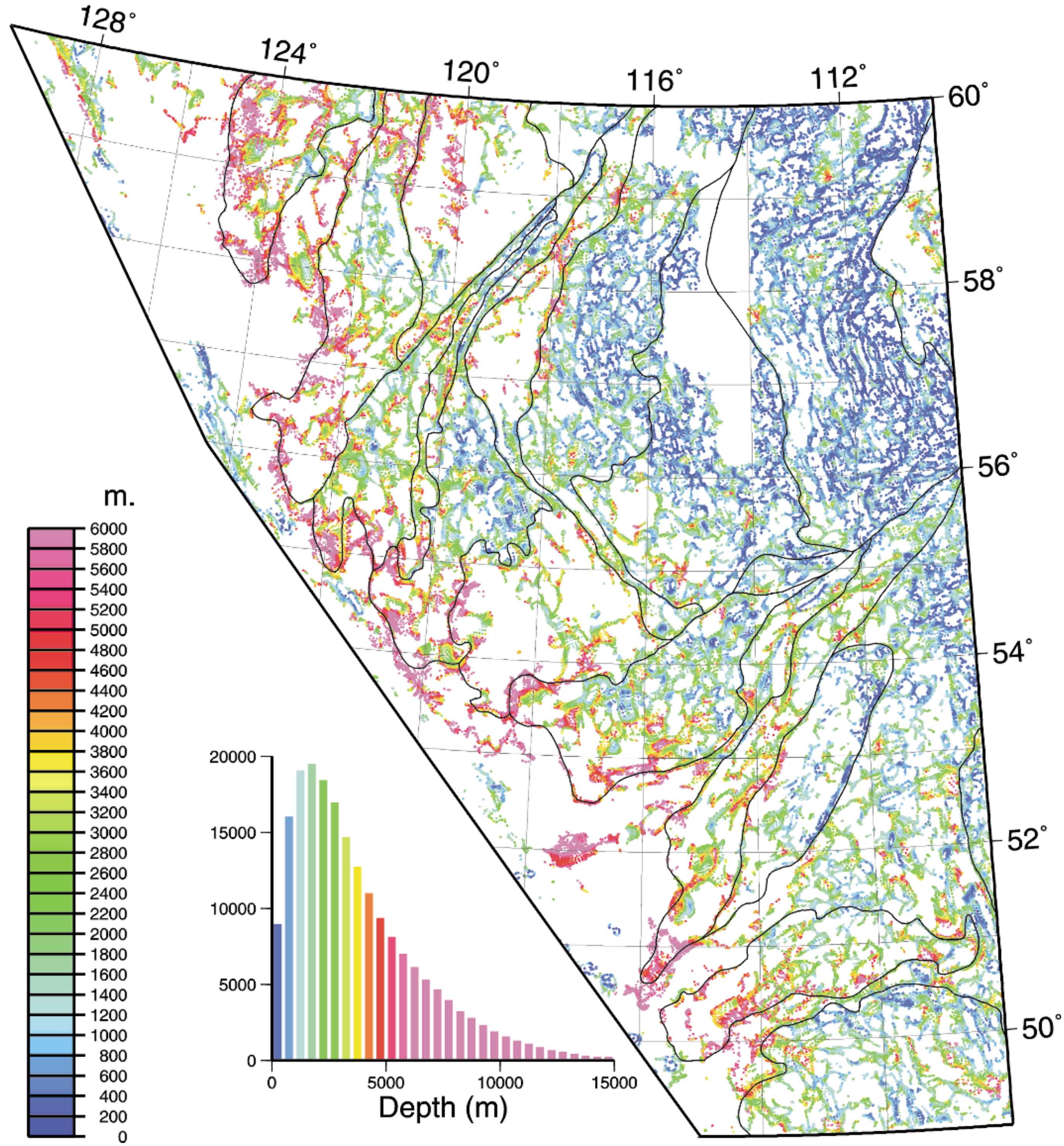

shows the mapped positions of analytic signal maxima derived from the draped magnetic data (Fig. 7).

Trend directions

Quantitative measures of anomaly trend directions within each domain were derived from the gradient maps already available. Anomaly strikes were estimated by fitting a plane, in a least-squares sense, to a 6.4 × 6.4 km grid-cell moving window applied to the pseudo-gravity and horizontal gravity gradient maps. This resulted in a strike direction value at every grid point. Strike directions were then extracted at grid points corresponding to the maxima locations (Figs. 10*b*, 10*c*) for each of the domains. Figures 11 and 12 show trend direction plots for the magnetic and gravity maps, respectively. In the north, magnetic trends show a consistent, generally northerly orientation that changes to a well-defined

Fig. 10. (*a*) Pseudo-gravity gradient maxima. (*b*) Horizontal magnetic gradient maxima. (*c*) Horizontal gravity gradient maxima. (*d*) Analytic signal maxima. Solid grey lines denote interpreted domain boundaries. Longer dashed line is the Cordilleran deformation front. Shorter dashed line is the edge of the Phanerozoic.

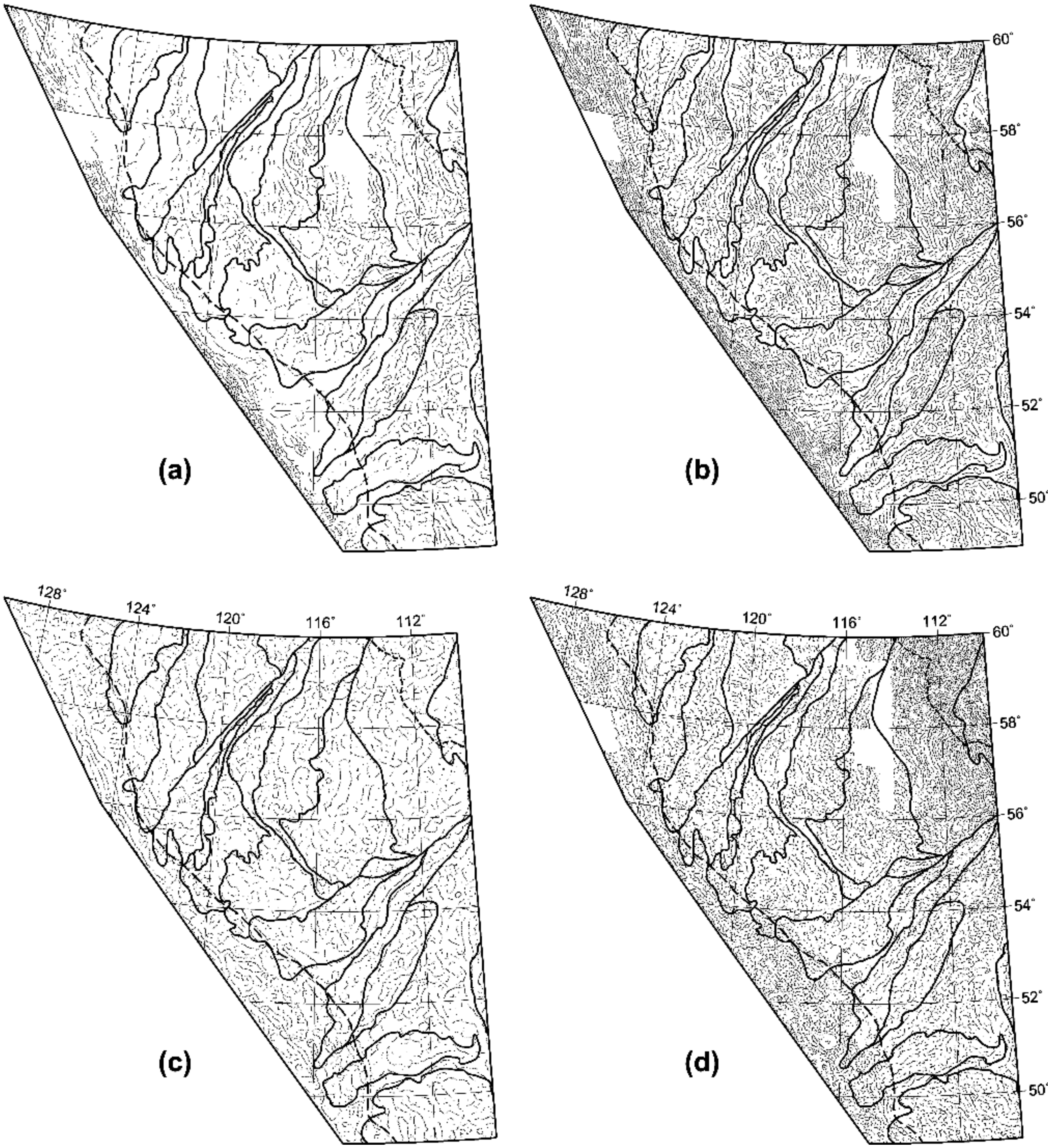

northeasterly direction south of the Snowbird tectonic zone (Fig. 8). This, in turn, gives way to the well-defined northwesterly strike of the Medicine Hat block. Gravity anomalies exhibit similar behaviour, but their trends have more scatter within most domains, especially in the north. Away from the Cordilleran deformation front, the gravity field north of the Snowbird tectonic zone is characterized by a prevalent northerly trend changing to a well-defined northeasterly orientation in the south, which is, in turn, terminated by the northwesterly trending Medicine Hat block. The Cordilleran deformation front imposes a northwesterly grain on those domains in the west close to the Rocky Mountains (cf. Fig. 5), reflecting density variations within northwest-striking thrust sheets.

Magnetizations

Cores from 300 basement intersections have been analyzed for rock properties by Burwash (1957), and Burwash

Table 1. Characteristics of basement domains of Alberta and northeastern British Columbia.

Domain	Age (Ga)	Type	Average anomaly (nT)	Standard deviation (nT)	Amplitude	Average trend	Magnetic character
Fort Nelson	?	Arc?	451	303	Very high	NNE	Smooth; few linear trends.
Nahanni	?	?	–28	95	Variable, mostly low	NNW	Smooth; few linear trends.
Fort Simpson	1.8	Arc	283	155	High	N	Generally smooth; few NNW trends in centre, NNE in south.
Hottah	1.8–1.9	Accreted terrane	–203	148	Low	NNW	Smooth; few E to NE highs due to dykes.
Nova	2.0–2.8	Archean	240	182	Variable high to moderate	NNE	Variable grain; ovoid NNE trends in south, lineated NNW in north.
Ksituan	1.9–2.0	Arc	426	234	High	N	Variable; lineated NE in north, lower amplitude ovoid in south.
Buffalo Head (High)	2.0–2.3	Accreted terrane	294	235	High	NNE	Well-defined striated fabric, convex to west.
(Utikuma)	—	—	72	201	Variable, high to low	NNW	Striated in north and east, ovoid in south and west.
Talston	1.9	Arc	172	279	Variable, high to low	NNW	Short wavelength, ovoid in north. Lineated NNE trends in south.
Great Bear	1.7–1.9	Arc	175	147	Variable, high to low	None	Variable linear trends.
Kiskatinaw	1.9–2.0	?	– 48	180	Low	N	Few N trends parallel to boundaries.
Chinchaga	2.1–2.2	?	–112	151	Low	N	NNE–NNW low-amplitude trends, less well-defined in south.
Wabamun	2.3	Accreted terrane	187	194	Variable, high to low	None	Strong subcircular anomalies. No linear trends.
Thorsby	1.9–2.4	?	–107	96	Low	NE	Well-defined, but few low-amplitude NE trends, parallel to boundaries.
Rimbey	1.8	Arc	144	126	Variable, moderate to low	NE	Well-defined, lineated NE trends, parallel to boundaries.
Lacombe	?	?	96	127	Variable, high to low	NE	Well-defined, short-wavelength NE trends, lineated, parallel to boundaries.
Loverna	1.8–2.7	Archean	–6	127	Variable, moderate to low	None	Generally subcircular highs. Trends variable, N to E.
Eyehill	2.6	Archean	395	240	High	N	Well-defined N trends (mostly in west).
Matzhiwin	2.5	Archean	217	144	High	ENE	Lineated fabric with moderate-amplitude ENE trends.
Vulcan	2.6	Archean	—	—	Low	ENE	Few N to E trends following domain edges. Generally lineated.
Medicine Hat	2.6–3.2	Archean	114	200	Variable, moderate to low	NW	Lineated NNW and NW trends, turning W farther north.

Note: Ages and domain type from Ross et al. (1991) and Villeneuve et al. (1993).

and Burwash (1989). Eighty percent of these samples occur in the Buffalo Head domain, while many other domains have very few (<10) intersections. Buffalo Head samples (total of 241) give an average susceptibility of 0.0024 SI (equivalent to a 0.12 $A \cdot m^{-1}$ magnetization in a 60 000 nT inducing field), while 13 samples from the Ksituan domain show an average of 0.0114 SI (0.57 $A \cdot m^{-1}$). Such small numbers of samples are unlikely to be representative of the bulk or average magnetic properties within the domains since susceptibility is highly variable both laterally and vertically. Therefore, modelling was carried out on profiles across the domains. In this fashion, estimates of magnetization can be made over much larger volumes and more meaningful bulk property values derived. Since the modelling is unconstrained at depth, exact geometries are not very reliable and (or) informative and are not shown here. However, the derived magnetizations are less sensitive to geometrical variations in modelled sources and can be useful in making some broad comparisons. Again, for modelling purposes, the effects of only induced magnetization were considered.

Several domains can be accounted for with modelled magnetizations of zero, implying that magnetic sources within these domains are paramagnetic, that is, they comprise low-susceptibility silicate minerals, such as biotite, olivine, and amphiboles, which have susceptibilities <0.002–0.005 SI (cf. Henkel 1994; Korhonen et al. 1997). The

Fig. 11. Rose diagrams of strike directions from magnetic data.

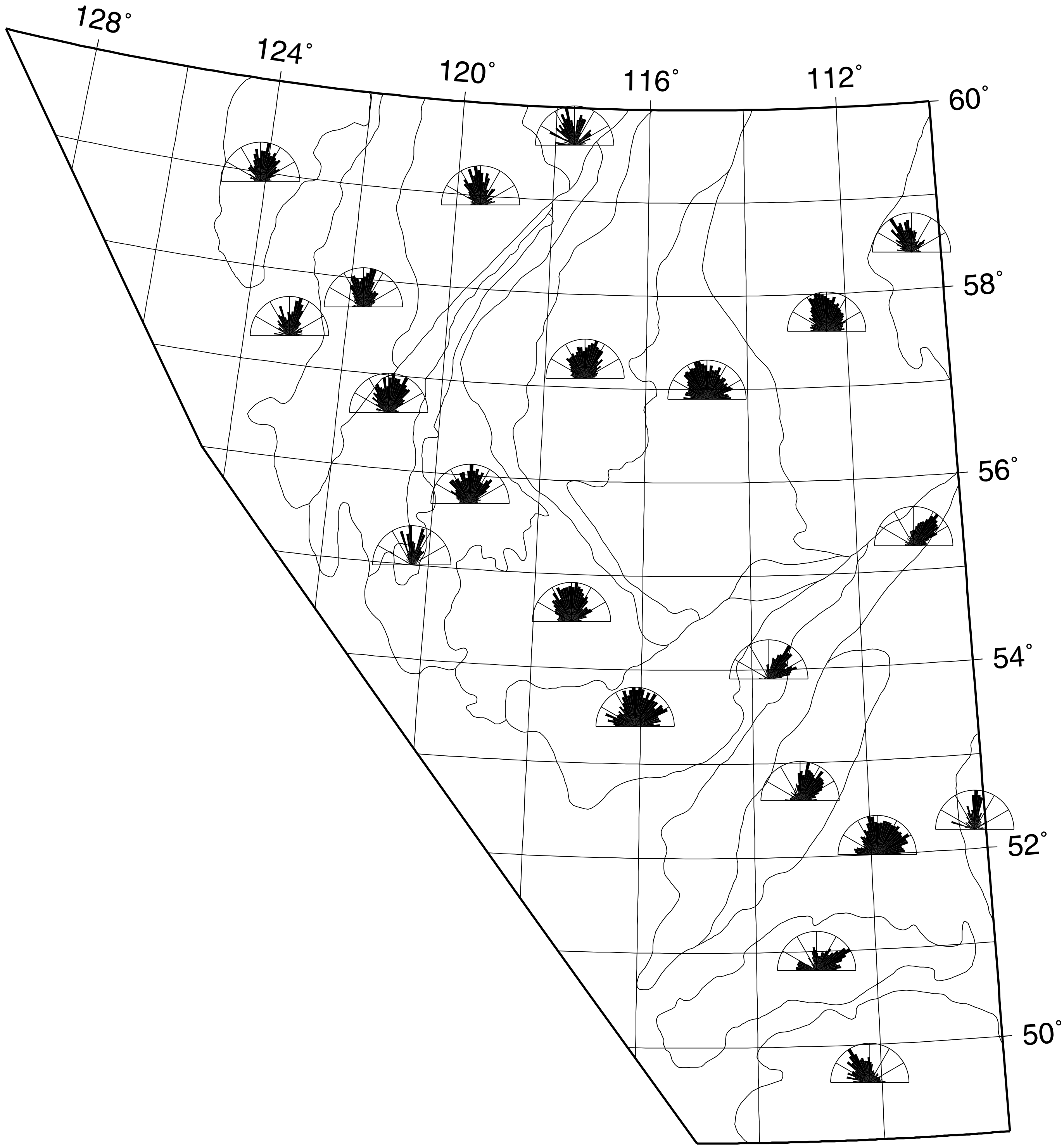

Nahanni, Hottah, Chinchaga, Thorsby, Vulcan, and Kiskatinaw domains (Fig. 8) make up this class. Lithologies that are consistent with such low magnetizations are S-type granites, paragneiss, and paramagnetic varieties of granitoid and basic rocks. Ilmenite-bearing plutonic rocks also may not have sufficiently high magnetizations to produce anomalies at regional scales. All other domains are characterized by the presence of ferrimagnetic material, most likely magnetite, which has a sufficiently high susceptibility to produce measurable anomalies. The highest magnetizations are found in the Fort Nelson, Fort Simpson, Buffalo Head, Talston, Ksituan, and Matzhiwin domains (Fig. 8), with values generally up to 5 $A \cdot m^{-1}$ (the Fort Nelson domain is exceptional with estimated values of up to 10 $A \cdot m^{-1}$). Such large magnetizations are usually indicative of intermediate igneous rocks associated with magmatic-arc environments. Mod-

Fig. 12. Rose diagrams of strike directions from gravity data.

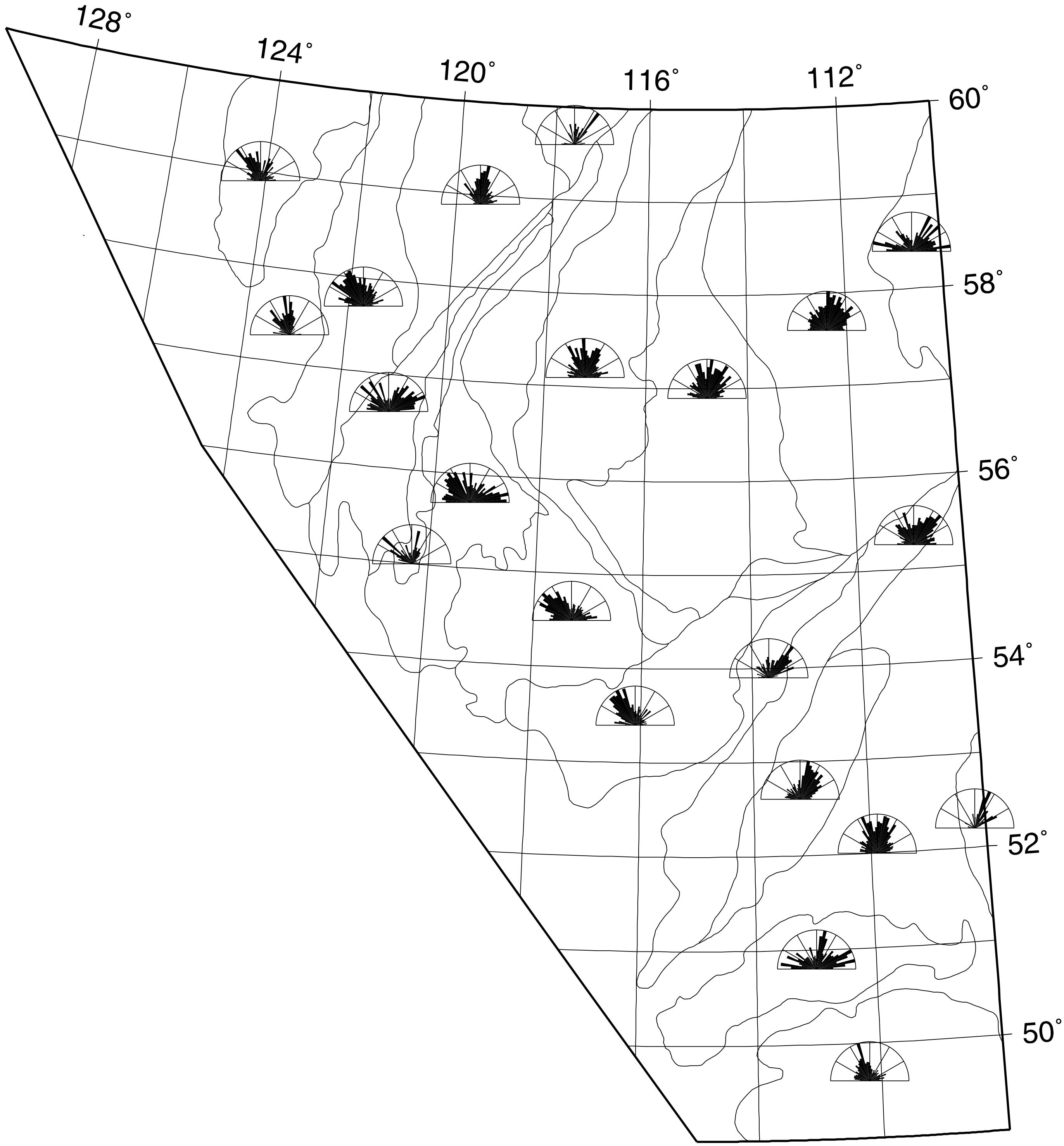

erate magnetizations up to 3 $A \cdot m^{-1}$ are characteristic of the Nova, Wabamun, Lacombe, Rimbey, Loverna, and Medicine Hat domains (Fig. 8), suggesting the presence of ferrimagnetic basic and granitoid rocks, orthogneiss, and intermediate volcanic rocks. Within some of the moderately magnetic domains are areas of paramagnetic lithologies which produce no magnetic anomalies.

Discussion

The techniques outlined above gave consistent results as to source locations within the Western Canada Sedimentary Basin (Figs. 9, 10) indicating a relatively uncomplicated magnetic source configuration. However, we note that in the results of all these methods, the derived locations of source bodies can be influenced by nearby source effects. The main difference between the delineations of Fig. 8 and previous interpretations is the extension of domains further to the southwest, due mainly to the availability of new public-domain magnetic data and the more precise definition of domain boundaries based on the magnetic source location maps. Domain definition is based on anomaly and inferred source trends, amplitudes, and wavelengths. Where anomaly trends and magnitudes are poorly defined, such as low-amplitude areas in the deepest part of the basin, maps of upward continued (emphasizing long wavelength components) versions of the magnetic data have been used to define domain extents based mainly on average amplitudes.

Ross et al. (1991) inferred domain boundaries by using the zero contour of the residual magnetic field intensity as an indicator of magnetic source body edges. The error in using the zero contour versus the true body edge is ~20% of the depth to the source for vertically sided bodies. This is not expected to produce appreciable differences at the scale of the figures shown here. Greater discrepancies will arise for dipping structures, where, for a given dip, the ratio of the difference between the zero contour and the body edge versus the depth is larger for shallower sources. However, the most significant differences between the boundaries of Fig. 8 and those of Ross et al. (1991) result from the choice of the individual anomaly that is assigned to mark each domain edge. Where domains have similar strikes, such as in southern Alberta, and consist of a striated fabric with alternating anomaly highs and lows, some latitude exists in the positioning the boundary, even when average amplitudes over domain-sized areas are taken into account. Differences in position range up to >20 km in these cases. For boundaries between two domains having dissimilar trends, differences between the two maps are usually <10 km.

At regional scales in the exposed Canadian Shield, the correlation between magnetic highs and calc-alkaline magmatic-arc rocks has been established based on mapped geology (Hoffman 1989) and magnetic properties of surface samples (Henderson et al. 1990; Pilkington and Percival 1999). As noted by Villeneuve et al. (1993), the interpretation of magnetic lows is not so straightforward. As mentioned earlier, modelling of profiles over domains exhibiting magnetic lows in the WCSB showed these domains are effectively nonmagnetic, that is, any iron present is in the form of paramagnetic Fe-silicates. The question is, however, what is the origin of these low magnetization zones. By analogy with several well-defined regional magnetic lows in exposed shield areas, the cause may be related to destruction of ferrimagnetic minerals as a result of deformation and metamorphism at collisional domain boundaries. For example, regional magnetic lows occur over the eastern and western edges of the Slave Province and the Grenville Front tectonic zone (e.g., Thomas 1992; Zheng and Arkani-Hamed 1998). Several petrological studies detail the reactions that result in a decrease in magnetic mineral content accompanying collisional processes. Haggerty (1979) noted that, in general, metamorphism and coupled metasomatism in igneous rocks tend to result in the breakdown of magnetic oxide minerals into paramagnetic sphene, amphibole, pyroxene, and secondary phyllosilicates. Hageskov (1984) mapped decreased susceptibilities in diabase dykes that correlated with increased deformation and metamorphic grade, due to the alteration of titanomagnetite to sphene and Fe-silicates. Recrystallization led to smaller grain sizes, which also caused a reduction in magnetization. Toft et al. (1993) suggested that decreases in magnetization in rocks from the Grenville Front, due to deformation-related hydration of Fe-Al-Cr-Ti-oxides to amphibole and rutile, may explain magnetic lows over continental collision zones. Whitaker (1994) documented a 10–50 km wide reworked zone characterized by low magnetizations caused by deformation and metamorphism in the Yilgarn block in western Australia at the boundary with the Albany block to the south. Other examples of magnetic lows at geophysical domain boundaries in Australia are given in Wellman (1998), who noted that these zones usually occur over distances up to 100 km perpendicular to strike.

The narrower regions of magnetic lows, such as the Thorsby, Kiskatinaw, and Vulcan domains, are therefore expected to result from such demagnetization effects accompanying collision. Since demagnetization zones are limited in extent (Thomas 1992; Shaw et al. 1996; Wellman 1998), the wider, more extensive magnetic lows of the Chinchaga and Hottah domains likely result from a combination of boundary demagnetization and a lower bulk magnetization level of crustal lithologies present. Basement samples from the Hottah domain consist of syenogranite, felsic gneiss, and tonalite, which tend to have low magnetizations, although holes drilled through the Chinchaga domain intersected granitic gneiss and quartz monzonite that are usually quite magnetic. Susceptibility values from Burwash (1957) and Burwash and Burwash (1989) do support low magnetizations, with average susceptibilities of 0.000133 and 0.000094 SI for the Chinchaga and Hottah domains, respectively. However, the much lower than modelled susceptibilities measured for samples from the Ksituan magmatic arc and Buffalo Head domains highlight the question of how representative these values are. Nonetheless, the presence of extensive magnetic lows indicate consistently lower magnetizations throughout the crust constituting these domains, reflecting differences in the mode of formation and (or) origin compared to the surrounding (more magnetic) domains. By analogy with domains in the Superior Province, magnetic lows could comprise dominantly metasedimentary and (or) volcanic basement as opposed to more magnetic plutonic domains.

The possibility of remanent magnetization in a direction opposing the present-day geomagnetic field could also contribute to the negative magnetic anomalies. However, based on the arguments presented earlier, it is unlikely that coherent remanence directions exist over domain-sized areas. The domain magnetic lows can be explained simply as the dipolar effects resulting from the juxtaposition of paramagnetic and ferrimagnetic basement blocks. This is borne out by previous modelling at collisional boundaries. Teskey and Hood (1991) demonstrated that the magnetic low at the boundary of the Slave Province and Thelon tectonic zone could be modelled as the negative portion of the associated magnetic high caused by the Thelon magmatic arc. Similarly, Hall et al. (1985) showed how the dipolar anomaly associated with the Superior–Hearne provinces boundary in

Manitoba could be explained in terms of a step in a magnetized crustal layer. In both these cases, the sources of magnetization are deep, at mid- to lower crustal depths, which supports the lack of correlation between surface geology and the associated anomaly lows noted at these boundaries (Thomas 1992).

Comparison of the gravity and magnetic data and their enhancements shows that mapped density and magnetization contrasts are not coincident, that is, the sources of the two types of anomalies are different. As discussed above, we expect the majority of the magnetic signal to be caused by magnetization changes at or near to the basement surface. The gravity signal, on the other hand, reflects the sum of contributions from density contrasts within the sedimentary section, where present, and the crystalline crust, the crust–mantle boundary, and within the mantle. The generally poor correlation between gravity and magnetic trends in the WCSB contrasts strongly with the situation in Australia (Shaw et al. 1996; Wellman 1998) and at larger scales within Canada, where coincident trends are found at geological province boundaries (e.g., Thomas 1992). Within the WCSB, only the Snowbird tectonic zone and the Vulcan anomaly (Fig. 8) have associated gravity and magnetic signatures. It is possible that the difference in scale between the domains defined here (Fig. 8) and those with greater dimensions could play a role in the type of anomaly occurring at domain boundaries. At smaller scales, the effect of intracrustal density contrasts, due to large plutonic complexes and major structures, may be comparable to contrasts between adjacent domains. Additionally, the coincident magnetic and gravity signatures of the Snowbird tectonic zone and the Vulcan anomaly likely indicate the significance of these crustal boundaries compared to those only associated with magnetization changes. Seismic data over the former boundaries indicate fundamental changes in crustal structure (Ross et al. 1995; Clowes et al. 1997) that most likely are accompanied by lateral variations in density throughout the whole crust.

Acknowledgments

Mike Thomas is thanked for useful comments on an earlier version of the manuscript. Helpful journal reviews were provided by Leo Nadeau and an anonymous reviewer.

References

Adams, D.C., and Keller, G.R. 1996. Precambrian basement geology of the Permian basin region of west Texas – eastern New Mexico: a geophysical perspective. American Association of Petroleum Geologists Bulletin, **80**: 410–431.

Arkani-Hamed, J., and Celetti, G. 1989. Effects of thermal remanent magnetization on the magnetic anomalies of intrusives. Journal of Geophysical Research, **94**: 7364–7378.

Burwash, R.A. 1957. Reconnaissance of subsurface Precambrian of Alberta. Bulletin of the American Association of Petroleum Geologists, **41**: 70–103.

Burwash, R.A., and Burwash, R.W. 1989. A radioactive heat generation map for the subsurface Precambrian of Alberta. *In* Current research, part C. Geological Survey of Canada, Paper 89-1C, pp. 363–368.

Cady, J.W. 1989. Geologic implications of topographic, gravity, and aeromagnetic data in the northern Yukon–Koyukuk province and its borderlands, Alaska. Journal of Geophysical Research, **94**: 15 821 – 15 841.

Clark, D.A. 1997. Magnetic petrophysics and magnetic petrology: aids to geological interpretation of magnetic surveys. Australian Geological Survey Organisation, Journal of Geology and Geophysics, **17**: 83–104.

Clowes, R., Hammer, P., Mandler, H., Ross, G., Cook, F., and Eaton, D. 1997. The Vulcan low, Matzhiwin high and related domains as revealed by SALT 95 reflection data. *In* Report of Lithoprobe Alberta Basement transects workshop. *Edited by* G.M. Ross. Lithoprobe Report No. 59, pp. 15–22.

Coles, R.L., Haines, G.V., and Hannaford, W. 1976. Large scale magnetic anomalies over western Canada and the Arctic: a discussion. Canadian Journal of Earth Sciences, **13**: 790–802.

Cook, F.A., Varsek, J.L., and Thurston, J.B. 1995. Tectonic significance of gravity and magnetic variations along the Lithoprobe southern Canadian Cordillera transect. Canadian Journal of Earth Sciences, **32**: 1584–1610.

Cordell, L.E., and Grauch, V.J.S. 1985. Mapping basement magnetization zones from aeromagnetic data in the San Juan Basin, New Mexico. *In* The utility of regional gravity and magnetic anomaly maps. *Edited by* W.J. Hinze. Society of Exploration Geophysicists, pp. 181–197.

Hageskov, B. 1984. Magnetic susceptibility used in mapping of amphibolite facies recrystallisation in basic dykes. Tectonophysics, **108**: 339–351.

Haggerty, S.E. 1979. The aeromagnetic mineralogy of igneous rocks. Canadian Journal of Earth Sciences, **16**: 1281–1293.

Hall, D.H., Noble, I.A., and Millar, T.W. 1985. Crustal structure of the Churchill–Superior boundary zone between 80° and 98°W longitude from Magsat anomaly maps and stacked passes. Journal of Geophysical Research, **90**: 2621–2630.

Henderson, J.B., McGrath, P.H., Theriault, R.J., and van Breemen, O. 1990. Intracratonic indentation of the Archean Slave Province into the Early Proterozoic Thelon Tectonic Zone of the Churchill Province, northwestern Canadian Shield. Canadian Journal of Earth Sciences, **27**: 1699–1713.

Henkel, H. 1994. Standard diagrams of magnetic properties and density — a tool for understanding magnetic petrology. Journal of Applied Geophysics, **32**: 43–53.

Hildenbrand, T.G. 1985. Magnetic terranes in the central United States determined from the interpretation of digital data. *In* The utility of regional gravity and magnetic anomaly maps. *Edited by* W.J. Hinze. Society of Exploration Geophysicists, pp. 248–266.

Hoffman, P.F. 1989. Precambrian geology and tectonic history of North America. *In* The geology of North America – an overview. *Edited by* A.W. Bally and A.R. Palmer. Geological Society of America, The geology of North America, Vol. A, pp. 447–512.

Johnson, P.R., and Stewart, I.C.F. 1995. Magnetically inferred basement structure in central Saudi Arabia. Tectonophysics, **245**: 37–52.

Korhonen, J.V., Säävuori, H., and Kivekäs, L. 1997. Petrophysics in the crustal model program of Finland. *In* Current research 1995–1996. *Edited by* S. Autio. Geological Survey of Finland, Special Paper 23, pp. 157–173.

Leclair, A.D., Lucas, S.B., Broome, H.J., Viljoen, D.W., and Weber, W. 1997. Regional mapping of Precambrian basement beneath Phanerozoic cover in southeastern Trans-Hudson Orogen, Manitoba and Saskatchewan. Canadian Journal of Earth Sciences, **34**: 618–634.

McDonald, A.J.W., Fletcher, C.J.N., Carruthers, R.M., Wilson, D., and Evans, R.B. 1992. Interpretation of the regional gravity and magnetic surveys of Wales, using shaded relief and Euler deconvolution techniques. Geological Magazine, **129**: 523–531.

Percival, J.A., Mortensen, J.K., Stern, R.A., Card, K.D., and Bégin, N.J. 1992. Giant granulite terranes of northeastern Superior Province: the Ashuanipi complex and Minto block. Canadian Journal of Earth Sciences, **29**: 2287–2308.

Pilkington, M., and Percival, J.A. 1999. Crustal magnetization and long wavelength aeromagnetic anomalies of the Minto block, Quebec. Journal of Geophysical Research, **104**: 7513–7526.

Pilkington, M., and Roest, W.R. 1992. Draping aeromagnetic data in areas of rugged topography. Journal of Applied Geophysics, **29**: 135–142.

Pilkington, M., Roest, W.R., Kwan, K.C.H., and Dumont, R. 1995. Comparison of drape-flown and computationally draped aeromagnetic data in British Columbia. *In* Current research, part A. Geological Survey of Canada, Paper 1995-A, pp. 61–65.

Reid, A.B., Allsop, J.M., Granser, H., Millett, A.J., and Somerton, I.W. 1990. Magnetic interpretation in three dimensions using Euler deconvolution. Geophysics, **55**: 80–91.

Roest, W.R., Verhoef, J., and Pilkington, M. 1992. Magnetic interpretation using the 3-D analytic signal. Geophysics, **57**: 116–126.

Ross, G.M., Parrish, R.R., Villeneuve, M.E., and Bowring, S.A. 1991. Geophysics and geochronology of the crystalline basement of the Alberta Basin, western Canada. Canadian Journal of Earth Sciences, **28**: 512–522.

Ross, G.M., Milkereit, B., Eaton, D., White, D., Kanasewich, E.R., and Burianyk, M.J.A. 1995. Paleoproterozoic collisional orogen beneath the western Canada sedimentary basin imaged by Lithoprobe crustal seismic-reflection data. Geology, **23**: 195–199.

Schlinger, C.M. 1985. Magnetization of the lower crust and interpretation of regional magnetic anomalies: an example from Lofoten and Vesterålen, Norway. Journal of Geophysical Research, **90**: 11 484 – 11 504.

Shaw, R.D., Wellman, P., Gunn, P.J., Whitaker, A.J., Tarlowski, C., and Morse, M. 1996. Guide to using the Australian crustal elements map. Australian Geological Survey Organisation, Record 1996/30.

Shive, P.N. 1989. Can remanent magnetization in the deep crust contribute to long wavelength magnetic anomalies? Geophysical Research Letters, **16**: 89–92.

Sprenke, K.F., and Kanasewich, E.R. 1982. Gravity modelling and isostasy in Western Canada. Journal of the Canadian Society of Exploration Geophysicists, **18**: 49–57.

Stephenson, R.A., Zelt, C.A., Ellis, R.M., Morel-a-l-Huissier, P., Mereu, R.F., Northey, D.J., West, G.F., and Kanasewich, E.R. 1989. Crust and upper mantle structure and the origin of the Peace River Arch. Bulletin of Canadian Petroleum Geology, **37**: 224–235.

Teskey, D.J., and Hood, P.J. 1991. The Canadian aeromagnetic database: Evolution and applications to the definition of major crustal boundaries. Tectonophysics, **192**: 41–56.

Thomas, M.D. 1992. Ancient collisional continental margins in the Canadian Shield; geophysical signatures and derived crustal transects. *In* Basement tectonics 8: characterization and comparison of ancient and Mesozoic continental margins. Proceedings of the 8th International Conference on Basement Tectonics. *Edited by* M.J. Bartholomew, D.W. Hyndman, D.W. Mogk, and R. Mason. Kluwer, Dordrecht, The Netherlands, pp. 5–25.

Thomas, M.D., Grieve, R.A.F., and Sharpton, V.L. 1988. Gravity domains and the assembly of the North American continent by collisional tectonics. Nature, **331**: 333–334.

Toft, P.B., Scowen, P.A.H., Arkani-Hamed, J., and Francis, D. 1993. Demagnetization by hydration in deep-crustal rocks in the Grenville Province of Quebec, Canada: Implications for magnetic anomalies of continental collision zones. Geology, **21**: 999–1002.

Villeneuve, M.E., Ross, G.M., Parrish, R.R., Theriault, R.J., Miles, W., and Broome, J. 1993. Geophysical subdivision, U–Pb geochronology and Sm–Nd isotope geochemistry of the crystalline basement of the Western Canada Sedimentary Basin, Alberta and northeastern British Columbia. Geological Survey of Canada, Bulletin 447.

Wadge, G., and Snoke, A.W. 1991. Images of the edges of aeromagnetic anomalies as an aid to geological mapping: the case history of Tobago, West Indies. Surveys in Geophysics, **12**: 515–530.

Watkins, N.D. 1961. The relative contributions of remanent and induced magnetism to the observed magnetic field in northeast Alberta. Geophysical Prospecting, **9**: 421–426.

Wellman, P. 1985. Block structure of continental crust derived from gravity and magnetic maps, with Australian examples. *In* The utility of regional gravity and magnetic anomaly maps. *Edited by* W.J. Hinze. Society of Exploration Geophysicists, pp. 102–108.

Wellman, P. 1998. Mapping of geophysical domains in the Australian crust using gravity and magnetic anomalies. *In* Structure and evolution of the Australian continent. *Edited by* J. Braun, J. Dooley, B. Goleby, R. van der Hilst, and C. Klootwijk. American Geophysical Union, Geodynamics Series 26, pp. 59–71.

Whitaker, A. 1994. Integrated geological and geophysical mapping of southwestern Western Australia. Australian Geological Survey Organisation, Journal of Geology and Geophysics, **15**: 313–328.

Zheng, Y., and Arkani-Hamed, J. 1998. Joint inversion of gravity and magnetic anomalies of eastern Canada. Canadian Journal of Earth Sciences, **35**: 832–853.